Journal of Medicinal Chemistry Article

J. Med. Chem. **2010,** *53,* 5333–5341 **5333**
DOI: 10.1021/jm100623e

^{68}Ga-Labeled Inhibitors of Prostate-Specific Membrane Antigen (PSMA) for Imaging Prostate Cancer

Sangeeta Ray Banerjee, Mrudula Pullambhatla, Youngjoo Byun, Sridhar Nimmagadda, Gilbert Green, James J. Fox, Andrew Horti, Ronnie C. Mease, and Martin G. Pomper*

Russell H. Morgan Department of Radiology and Radiological Sciences, Johns Hopkins Medical Institutions, 1550 Orleans Street, Baltimore, Maryland 21231

Received May 21, 2010

Gallium-68 is a generator-produced radionuclide for positron emission tomography (PET) that is being increasingly used for radiolabeling of tumor-targeting peptides. Compounds [^{68}Ga]**3** and [^{68}Ga]**6** are high-affinity urea-based inhibitors of the prostate-specific membrane antigen (PSMA) that were synthesized in decay-uncorrected yields ranging from 60% to 70% and radiochemical purities of more than 99%. Compound [^{68}Ga]**3** demonstrated 3.78 ± 0.90% injected dose per gram of tissue (%ID/g) within PSMA+ PIP tumor at 30 min postinjection, while [^{68}Ga]**6** showed a 2 h PSMA+ PIP tumor uptake value of 3.29 ± 0.77 %ID/g. Target (PSMA+ PIP) to nontarget (PSMA− flu) ratios were 4.6 and 18.3, respectively, at those time points. Both compounds delineated tumor clearly by small animal PET. The urea series of imaging agents for PSMA can be radiolabeled with ^{68}Ga, a cyclotron-free isotope useful for clinical PET studies, with maintenance of target specificity.

Introduction

Prostate cancer is the most commonly diagnosed malignancy and the second leading cause of cancer-related death in men in the United States.[1] In 2009, approximately 192,000 men were diagnosed with prostate cancer with 27,000 succumbing to the disease. The integral membrane protein prostate-specific membrane antigen (PSMA[a]) is becoming increasingly recognized as a viable target for imaging and therapy of prostate and other forms of cancer.[2,3]

Because of its similarity to Fe(III), Ga(III) complexes are emerging as an interesting alternative to Pt-based anticancer agents.[4−6] From a diagnostic standpoint, positron-emitting versions of Ga(III) can be used for tumor imaging.[7−9] Recently, the application of ^{68}Ga-labeled peptides has attracted considerable interest for cancer imaging because of the physical characteristics of ^{68}Ga.[10] ^{68}Ga is available from an in-house ^{68}Ge/^{68}Ga generator (^{68}Ge, $t_{1/2}$ = 270.8 day), which renders it independent of an on-site cyclotron. Therefore, ^{68}Ga-based PET agents possess significant commercial potential and serve as a convenient alternative to cyclotron-based isotopes for positron emission tomography (PET), such as ^{18}F or ^{124}I. ^{68}Ga has a high positron-emitting fraction (89% of its total decay). The maximum positron energy of ^{68}Ga (max energy = 1.92 MeV, mean = 0.89 MeV) is higher than that of ^{18}F (max = 0.63 MeV, mean = 0.25 MeV). However, a study of spatial resolution using Monte Carlo analysis revealed that under the assumption of 3 mm spatial resolution for most PET detectors, the full-width-at-half-maximum (FWHM) values of ^{18}F and ^{68}Ga are indistinguishable in soft tissue (3.01 mm vs 3.09 mm).[9] That finding implies that with the standard spatial resolution of 5−7 mm for current clinical scanners, image quality using ^{68}Ga-based radiotracers will likely be indistinguishable from that of ^{18}F-based agents, stimulating interest in the development of ^{68}Ga-labeled compounds for medical imaging.[7−9] With a physical half-life of 68 min, ^{68}Ga is also matched nicely to the pharmacokinetics of many peptides used for imaging. Furthermore, ^{68}Ga is introduced to biomolecules through macrocyclic chelators, which allows possible kit formulation and wide availability of the corresponding imaging agents.

We and others have previously demonstrated the ability to image PSMA-expressing prostate tumor xenografts with radiohalogenated, urea-based, low molecular weight inhibitors of PSMA.[11−15] Recently, we have extended that work to include the radiometal ^{99m}Tc via a coordinated, ^{99m}Tc tricarbonyl moiety.[16] To retain the binding affinity of those inhibitors to PSMA, a linker moiety was introduced between the amino functionalized PSMA urea and the metal chelator (Figure 1). A similar approach by Kularatne et al. produced ^{99m}Tc-oxo labeled inhibitors.[14,15] We have now extended this work further to include ^{68}Ga for PET imaging. Gallium(III) ion forms a stable complex (formation constant, log K_{ML} = 21.33) with the commercially available, widely used multidentate chelating agent, 1,4,7,10-tetraazacyclododecane-1,4,7,10-tetraacetic acid (DOTA).[17] This report describes the synthesis and in vitro binding of two new ^{68}Ga-labeled, conjugated PSMA inhibitors, [^{68}Ga]**3** and [^{68}Ga]**6** (Figure 1), as well the biodistribution and in vivo imaging studies of these compounds. The chelating agent we have employed is the triacetic acid monoamide of DOTA. Few ^{68}Ga-labeled, mechanism-based radiotracers for prostate cancer have been reported previously, and none for PSMA or that approach such low molecular weights as these.

*To whom correspondence should be addressed. Phone: 410-955-2789. Fax: 443-817-0990. E-mail: mpomper@jhmi.edu.

[a]Abbreviations: PSMA, prostate-specific membrane antigen; DCFBC, *N*-[*N*-[(*S*)-1,3-dicarboxypropyl]carbamoyl]-(*S*)-4-fluorobenzyl-L-cysteine; PMPA, 2-(phosphonomethyl)pentanedioic acid; DOTA, 1,4,7,10-tetraazacyclododecane-1,4,7,10-tetraacetic acid; PET, positron emission tomography.

Published on Web 06/22/2010

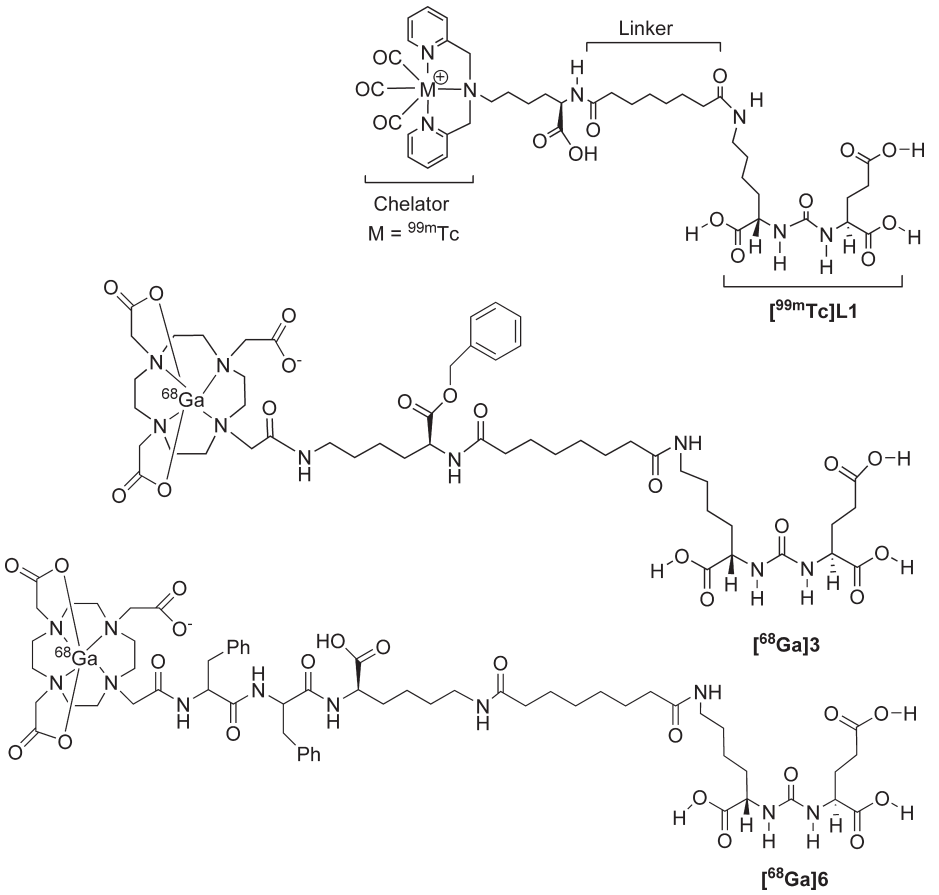

Figure 1. Urea-based PSMA ligands [^{99m}Tc]**L1**, [^{68}Ga]**3**, and [^{68}Ga]**6**.

Results

Chemical and Radiochemical Syntheses. DOTA-Conjugated Urea Inhibitors. Key *N*-hydroxysuccinimide (NHS) ester intermediate **1** (Scheme 1) was prepared following our previous report.[16] Compound **1** was then conjugated with the α-amine of H-Lys(Boc)-OBz[18] followed by simultaneous removal of Boc and PMB (*p*-methoxybenzyl) groups using a solution of trifluoracetic acid (TFA)/CH_2Cl_2 at 25 °C to produce **2**. The primary amine of **2** was then conjugated with DOTA-NHS (1,4,7,10-tetraazacyclododecane-1,4,7,10-tetraacetic acid mono(*N*-hydroxysuccinimide ester)) to obtain **3** in ~40% yield after purification by high-performance liquid chromatography (HPLC). NMR and mass spectrometry (MS) were used to confirm the identity of **3**.

Synthesis of DOTA conjugated PSMA inhibitor **6** was performed by using standard fluorenylmethoxycarbonyl (Fmoc) solid phase peptide synthesis (SPPS) starting from Fmoc-Lys(Boc)-Wang resin according to Scheme 2. After two phenylalanine residues were conjugated with the resin bound lysine, DOTA was conjugated at the N-terminal of the second phenylalanine residue after which the compound was cleaved from the resin by a 1:1 mixture of TFA/CH_2Cl_2 to produce **4**. The free ε-amine of lysine was then conjugated with **5**,[19] which was prepared from **1** by PMB cleavage to produce **6**. Compound **6** was characterized through standard spectroscopic techniques.

A stable gallium isotope (^{69,71}Ga) was introduced to the urea−DOTA conjugate by incubation of **3** or **6** with an aqueous solution of $GaCl_3$ at 95 °C for 10 min. Compounds [^{69,71}Ga]**3** and [^{69,71}Ga]**6** were characterized by standard spectroscopic analyses. The proposed structures of compounds [^{69,71}Ga]**3** and [^{69,71}Ga]**6**, as shown in Schemes 1 and 2 and Figure 1, were based on the reported X-ray crystal structures of gallium−DOTA compounds described by Maecke et al[20,21] and Doyle et al.[22] The mass spectra of the Ga compounds showed the expected isotope distribution pattern for natural gallium, which is a mixture ^{69}Ga (60.11%) and ^{71}Ga (39.89%).[23] The stable gallium-labeled conjugates were used as authentic reference material for the chromatographic analysis of the radiolabeling reactions to identify the corresponding ^{68}Ga-labeled compounds.

Radiochemistry. The ^{68}Ga(III) was eluted from the ^{68}Ge/^{68}Ga generator using ~6−7 mL of a solution of 0.1 N hydrochloric acid (HCl). To achieve high specificity radioactivity, radioactive material was preconcentrated and purified on a cation exchange resin following a literature method.[24] The ^{68}Ga(III) was eluted from the resin with 400 μL of an 97.6% acetone/0.05 N HCl mixture (pH, 2.30 ± 0.05) and was used immediately for aqueous radiolabeling of **3** and **6**. No buffer solution was added. The radiolabeling was performed at 90−95 °C for 10 min with decay-uncorrected yields ranging from 60% to 70% and radiochemical purities of more than 99%. On analysis of the reaction mixture by HPLC, the retention time of the radiolabeled compound was slightly longer than that of the corresponding free ligand. The specific radioactivity of purified [^{68}Ga]**3** and [^{68}Ga]**6** was between 3.0 and 6.0 MBq/nmol. The log $P_{\text{octanol/water}}$ values for [^{68}Ga]**3** and [^{68}Ga]**6** were approximately −3.9 as determined by the shake-flask method.[25] However, using an HPLC method, we found that the HPLC retention times for **6** (28 min) and [$^{69/71}$Ga]**6** (32 min) were longer than for **3** (19 min) and [$^{69/71}$Ga]**3** (24 min). It is evident that **6** and the corresponding gallium compound were more

Scheme 1[a]

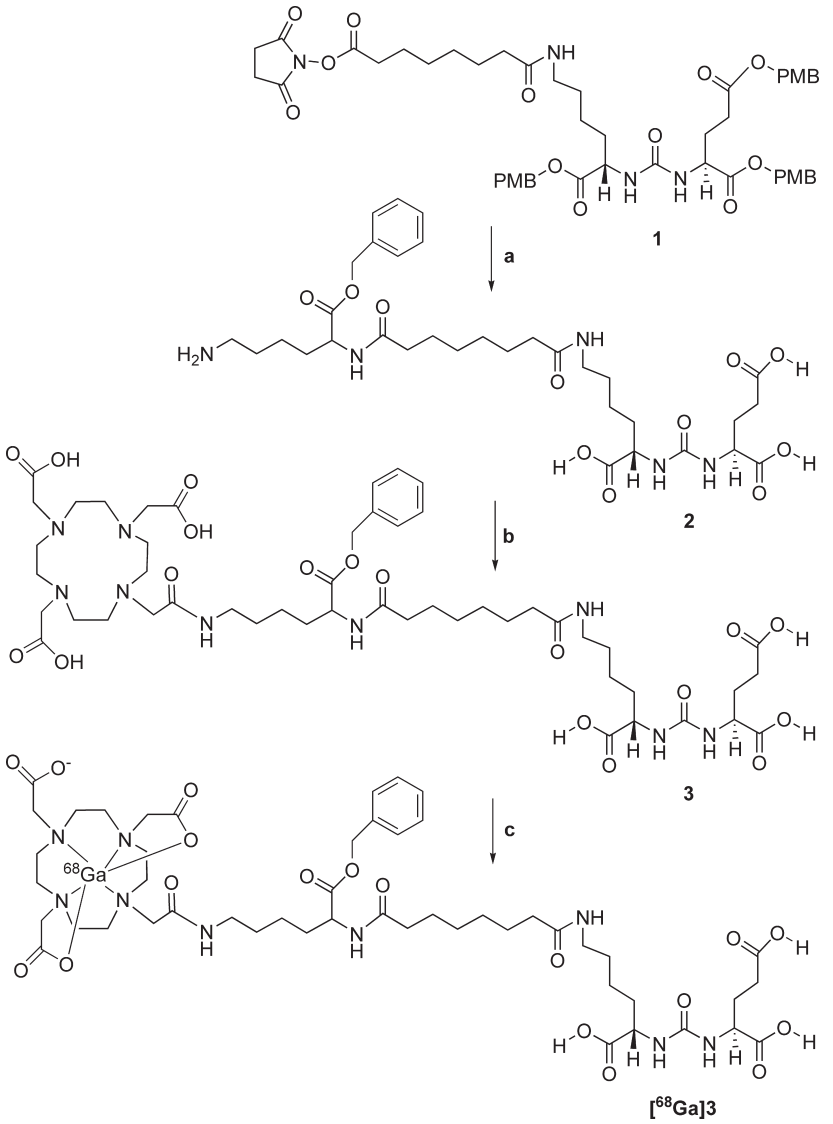

[a] (a) (i) H-Lys(Boc)-OBz, NEt_3, DMF, room temp, 16 h; (ii)TFA/CH_2Cl_2, room temp, 16 h; (b) DOTA-NHS, DMF,TEA, room temp, 16 h; (c) $GaCl_3$, water, pH 3.5, 90 °C.

lipophilic than **3** and its gallium-labeled analogue, which is reasonable in light of the presence of two phenylalanine residues in the long linker of **6**, while **3** has only one lysine residue protected as the benzyl ester. Interestingly, our previous lead compound, ^{99m}Tc**L1**,[16] was found to be much more lipophilic than either of these gallium compounds, with log $P_{\text{octanol/water}} \approx -3.1$, possibly because of its organometallic tricarbonyl core and the presence of the lipophilic bispyridyl chelating agent.

Biology. Cell Binding Assay. K_i values for **3**, [^{69,71}Ga]**3**, **6**, and [^{69,71}Ga]**6** were determined using a fluorescence-based PSMA inhibition assay.[26] All compounds were found to be potent inhibitors of PSMA, as we reported earlier for ^{99m}Tc**L1** and related compounds.[16] Compounds **3** and [^{69,71}Ga]**3** had inhibitory capacities of 2.9 and 29 nM, respectively. For **6** and [^{69,71}Ga]**6**, values were 1.23 and 0.44 nM, respectively.

Biodistribution. Compound [^{68}Ga]**3** was assessed for its pharmacokinetics ex vivo in severe-combined immunodeficient (SCID) mice bearing both PSMA+ PC3-PIP and PSMA− PC3-flu xenografts.[27] Table 1 shows the percent injected dose per gram (%ID/g) of radiotracer in selected organs for [^{68}Ga]**3**. Compound [^{68}Ga]**3** showed clear PSMA-dependent binding in PSMA+ PC3 PIP xenografts, reaching a maximum uptake of 3.78 ± 0.90 (SEM) %ID/g at 30 min postinjection (pi). The blood, spleen, and kidney displayed the highest uptake at 30 min. By 60 min, the urinary bladder showed the highest uptake; however, this uptake represents excretion at all time points. The high values noted in kidney are partially due to high expression of PSMA within proximal renal tubules.[28,29] Rapid clearance from the kidneys was demonstrated, decreasing from 97.19 ± 16.07 %ID/g at 30 min to 2.13 ± 0.11%ID/g at 3 h. The radioactivity in the PSMA+ PIP tumor cleared more slowly, from its aforementioned value at 30 min to 1.10 ± 0.19 %ID/g at 3 h.

Compound [^{68}Ga]**6** was also investigated for its pharmacokinetic characteristics in tumor-bearing mice at 5 min, 1 h, 2 h, and 3 h pi. Table 2 shows the %ID/g of radiotracer in selected organs for [^{68}Ga]**6**. As for [^{68}Ga]**3**, [^{68}Ga]**6** showed PSMA-dependent tumor uptake. After a peak, flow-related uptake at 5 min pi of 6.61 ± 0.55%, [^{68}Ga]**6** demonstrated a 2 h tumor uptake value of 3.29 ± 0.77%, which dropped to 1.80 ± 0.16% at 3 h. Uptake in blood was high at 5 min and

Scheme 2[a]

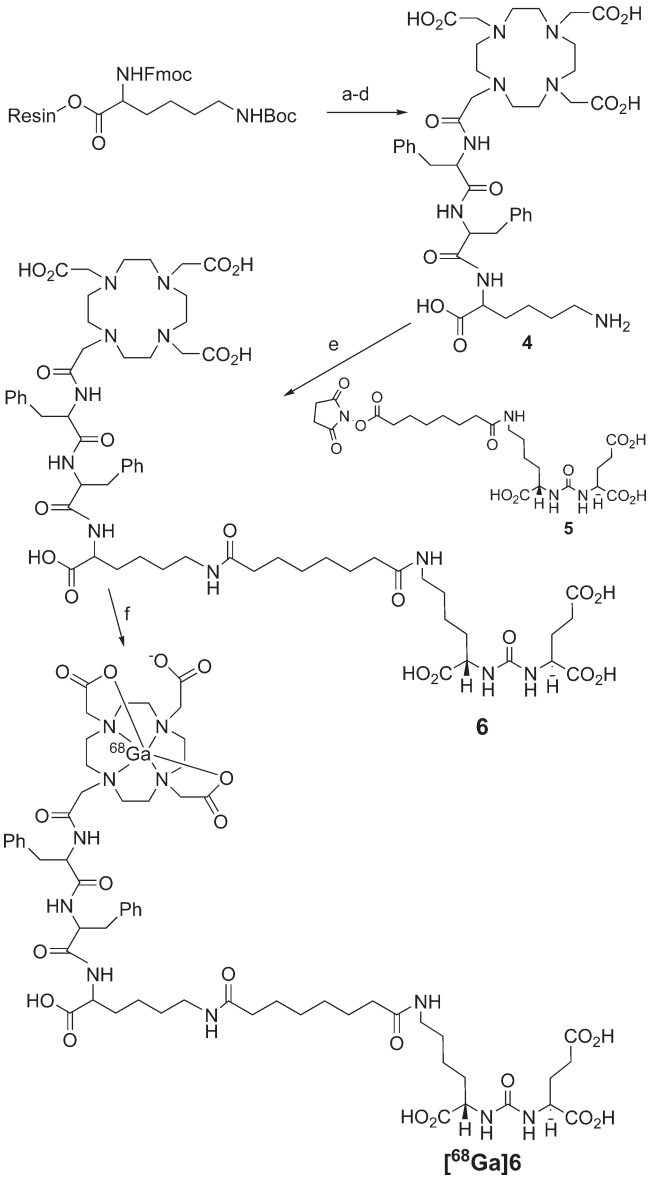

[a] (a) 20% piperidine in DMF, Fmoc-Phe-OH, HBTU, HOBT, DIEA, DMF; (b) 20% peridine in DMF, Fmoc-Phe-OH, HBTU, HOBT, DIEA, DMF; (c) 20% peridine in DMF, DOTA-tris(*tert*-butyl ester)-CO_2H, HBTU, HOBT, DIEA, DMF; (d) TFA, CH_2Cl_2, room temp, overnight; (e)TEA, DMF, room temp, overnight; (f) $^{68}GaCl_3$, pH 3.5, water, 90 °C, 10 min.

rapidly washed out within 1 h. Nontarget organs such as kidney, spleen, and lung showed high uptake at 5 min and rapidly washed out with time. With the exception of the kidneys and spleen, clearance from blood and normal organs was faster for [^{68}Ga]**6** than for [^{68}Ga]**3**. Again, high kidney uptake is associated with high expression of PSMA within proximal renal tubules.[28,29] Similar to [^{68}Ga]**3**, [^{68}Ga]**6** demonstrated faster clearance of radioactivity from kidney than from the PSMA+ tumor. However, the rate of clearance from kidney for [^{68}Ga]**6** was much slower than for [^{68}Ga]**3**, i.e., 65 ± 12% at 5 min pi and 10 ± 1.22% at 3 h.

Small Animal PET Imaging. Intense radiotracer uptake was seen only in the kidneys and tumor for both [^{68}Ga]**3** (Figure 2) and [^{68}Ga]**6** (Figure 3). As noted above for the ex vivo study, the intense renal uptake was partially due to specific binding of the radiotracer to proximal renal tubules[28,29] as well as to excretion of this hydrophilic compound. Apart from the kidneys, only the PSMA+ tumor demonstrated significant radiotracer uptake.

Table 1. Ex Vivo Tissue Biodistribution of [^{68}Ga]**3**

	biodistribution, %ID/g			
	30 min	60 min	120 min	180 min
blood	2.20 ± 0.90	1.93 ± 0.70	0.80 ± 0.30	0.62 ± 0.34
heart	0.70 ± 0.13	0.50 ± 0.08	0.21 ± 0.08	0.20 ± 0.02
liver	0.84 ± 0.24	0.83 ± 0.10	0.42 ± 0.0.07	0.50 ± 0.03
stomach	0.73 ± 0.13	0.75 ± 0.32	0.24 ± 0.07	0.24 ± 0.05
spleen	4.90 ± 1.10	3.35 ± 1.20	0.43 ± 0.19	0.32 ± 0.13
kidney	97.19 ± 16.07	64.68 ± 4.10	5.35 ± 2.12	2.13 ± 0.11
muscle	0.46 ± 0.16	0.25 ± 0.07	0.08 ± 0.04	0.05 ± 0.01
small intestine	0.79 ± 0.12	0.70 ± 0.34	0.26 ± 0.11	0.34 ± 0.20
large intestine	0.77 ± 0.14	0.95 ± 0.53	0.34 ± 0.10	0.46 ± 0.10
bladder	8.96 ± 5.30	25.29 ± 8.63	2.70 ± 4.02	5.39 ± 2.98
PC-3 PIP	3.78 ± 0.90	3.32 ± 0.33	1.31 ± 0.06	1.10 ± 0.19
PC-3 flu	0.82 ± 0.20	0.67 ± 0.08	0.41 ± 0.09	0.39 ± 0.02
PIP/flu	4.61	4.93	3.24	2.77
PIP/muscle	8.30	13.13	17.40	20.37
flu/muscle	1.80	2.67	5.37	7.34

Table 2. Ex Vivo Tissue Biodistribution of [^{68}Ga]**6**

	biodistribution, %ID/g			
	5 min	60 min	120 min	180 min
blood	6.28 ± 0.08	0.41 ± 0.05	0.15 ± 0.07	0.13 ± 0.01
heart	2.01 ± 0.24	0.19 ± 0.07	0.05 ± 0.03	0.03 ± 0.01
lung	4.59 ± 0.68	0.74 ± 0.54	0.20 ± 0.05	0.14 ± 0.03
liver	1.57 ± 0.16	0.24 ± 0.09	0.19 ± 0.03	0.14 ± 0.02
stomach	2.38 ± 0.35	0.38 ± 0.16	0.18 ± 0.02	0.04 ± 0.02
pancreas	1.52 ± 0.19	0.25 ± 0.14	0.08 ± 0.03	0.04 ± 0.02
spleen	5.17 ± 2.22	2.43 ± 1.07	0.78 ± 0.15	0.34 ± 0.09
fat	1.03 ± 0.02	0.40 ± 0.04	0.08 ± 0.02	0.02 ± 0.01
kidney	64.75 ± 12.00	26.57 ± 10.93	12.25 ± 1.79	10.04 ± 1.22
muscle	1.58 ± 0.33	0.12 ± 0.08	0.03 ± 0.02	0.00 ± 0.01
small intestine	2.04 ± 0.25	0.23 ± 0.05	0.09 ± 0.04	0.06 ± 0.03
large intestine	2.02 ± 0.49	0.50 ± 0.70	0.12 ± 0.03	0.12 ± 0.03
bladder	5.97 ± 1.50	7.65 ± 3.34	1.41 ± 1.17	0.75 ± 0.54
PC-3 PIP	6.61 ± 0.55	2.80 ± 1.32	3.29 ± 0.77	1.80 ± 0.16
PC-3 flu	2.63 ± 0.51	0.16 ± 0.08	0.18 ± 0.03	0.12 ± 0.03
PIP/flu	2.50	17.30	18.28	15.20
PIP/muscle	4.17	23.27	122.13	436.29
flu/muscle	1.67	1.34	6.68	28.70

Discussion

Because of its demonstrated clinical utility and the appearance of dual modality [PET/computed tomography (CT)] systems, clinical PET imaging has been accelerating worldwide and may soon become the dominant technique in nuclear medicine. PET isotopes tend to be short-lived and enable synthesis of "physiologic" radiotracers, namely, those that incorporate ^{15}O, ^{13}N, or ^{11}C, enabling precise conformity to the tracer principle. Being essentially isosteric to H, ^{18}F enables nearly tracer-level studies, with important caveats, particularly for [^{18}F]fluorodeoxyglucose (FDG), which is by far the most commonly used radiopharmaceutical for PET. But in part because FDG does not accumulate well within many tumor types,[30] including prostate cancer,[30,31] there has been a sustained effort in the development of radiometalated peptides, often employing ^{99m}Tc, that target G-protein-coupled receptors. Gallium-68 provides a link between PET and single photon emission computed tomography (SPECT), since metal chelating methodology needed for ^{99m}Tc can also be applied

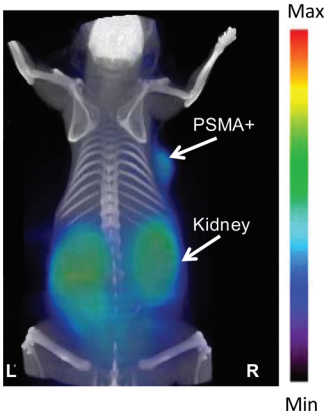

Figure 2. GE eXplore VISTA pseudodynamic PET image (co-registered with the corresponding CT image) of a PSMA+ LNCaP tumor-bearing mouse injected intravenously with 0.2 mCi (7.4 MBq) [^{68}Ga]**3**.

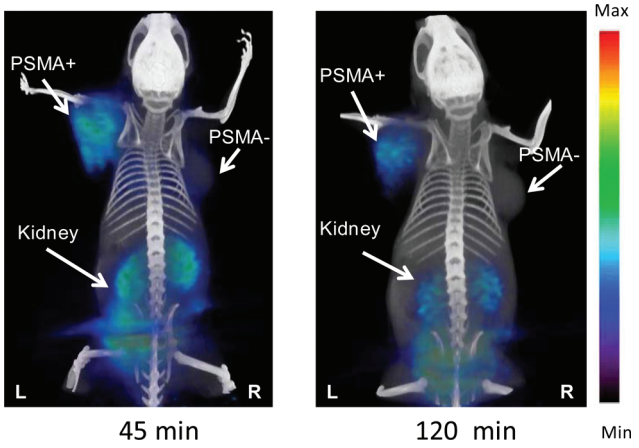

Figure 3. GE eXplore VISTA PET image (co-registered with the corresponding CT image) of a PSMA+ PIP and PSMA− flu tumor-bearing mouse injected intravenously with 0.2 mCi (7.4 MBq) [^{68}Ga]**6**.

to ^{68}Ga. A further analogy is the convenience of a ^{68}Ge/^{68}Ga generator (PET), as with ^{99}Mo/^{99m}Tc (SPECT), to provide readily available isotope, with no need for an in-house cyclotron. Although ^{18}F-labeled, low molecular weight PSMA inhibitors have shown promise in preclinical imaging studies,[13,32] the ready availability of generator-produced ^{68}Ga and the logical extension to PET from our published ^{99m}Tc-labeled series of PSMA-binding radiometalated imaging agents[16] provide the rationale for this study.

As for the ^{99m}Tc-labeled agents, the strategy we employed involves a tripartite imaging agent containing a PSMA targeting moiety, a linker, and a chelator for ^{68}Ga. The linker is necessary to enable productive binding by directing the ^{68}Ga-chelate complex through a 20 Å tunnel away from the active site. Because of its ability to chelate metals with a +3 oxidation state and its clinical track record, we used DOTA as the chelator for both [^{68}Ga]**3** and [^{68}Ga]**6**.[33−39] Both are also derived from a lysine−urea−glutamate construct that confers PSMA specificity. That still leaves significant structural differences, which are confined to the linker, between those two compounds. Those differences include two phenylalanines for [^{68}Ga]**6** relative to [^{68}Ga]**3**, while the latter compound possesses one benzyl-protected lysine within the linker. Because of the strict structural requirements of the S1′ (pharmacophore) pocket in which the glutamate moiety resides[40] and the need for at least one additional carboxylate (derived from lysine), modification of the linker is the best option to enable pharmacokinetic optimization of this series. A careful balance is sought whereby sufficient localization of the radiotracer to the tumor is needed, favoring higher hydrophobicity, while washout from nontarget sites such as liver and intestine is also desired, favoring higher hydrophilicity. The benzyl group was initially added to [^{68}Ga]**3** to provide a chromophore to facilitate purification, but the phenylalanines in [^{68}Ga]**6** were added to offset the high hydrophilicity of these compounds, potentially enabling longer and/or higher tumor sequestration, as originally proposed in a previous report.[14] The long retention times, while not necessary when using ^{68}Ga (physical half-life of 68 min), may be needed for longer lived isotopes, such as ^{111}In, or for therapeutic radiometals. However, even addition of two phenylalanines was not able to provide a compound as lipophilic as our previously published SPECT agent, ^{99m}Tc**L1**.

Figures 2 and 3 demonstrate the high target selectivity of [^{68}Ga]**3** and [^{68}Ga]**6** by delineating the PSMA+ tumors as well as kidney, which is a PSMA+ structure. Because we anticipate that most metastatic foci, for which these compounds are designed, will be in bone or lymph nodes (particularly those in pelvis), we do not anticipate that renal uptake will provide a significant confound for these agents. Although a PSMA-control tumor was not included in Figure 2, a separate blocking study was performed for [^{68}Ga]**3**, in which an animal pretreated with 50 mg/kg of the known PSMA-binding ligand, 2-(phosphonomethyl)pentanedioic acid (2-PMPA),[41] did not demonstrate PSMA+ tumor uptake (see Supporting Information), attesting to the binding specificity of this compound. The more quantitative ex vivo studies of [^{68}Ga]**3** and [^{68}Ga]**6** further support high PSMA target specificity, demonstrating target-to-nontarget (PIP/flu) ratios of approximately 5 and 18 at 1 and 2 h pi, respectively. The 1 and 2 h PSMA+ tumor uptake values for these compounds, 3.32 ± 0.33% and 3.29 ± 0.77%, respectively, for [^{68}Ga]**3** and [^{68}Ga]**6**, are comparable to other radiometalated PSMA inhibitors we have developed.[16] As shown in Figures 2 and 3 those values are sufficient for clear tumor imaging. Notably, PIP tumors contain about 1 order of magnitude lower PSMA than LNCaP tumors (data not shown), which are often employed to assess for binding specificity of PSMA-targeting agents. We generally prefer the PIP/flu comparison because both are derived from PC-3 cells, providing a more controlled study.

Conclusions

Compounds [^{68}Ga]**3** and [^{68}Ga]**6** demonstrate PSMA-specific tumor imaging in vivo. Because of higher target-to-nontarget ratios with comparable absolute uptake values to [^{68}Ga]**3**, [^{68}Ga]**6** will be pursued in additional animal models and for toxicity testing en route to clinical translation. In this manner we hope to add this cyclotron-independent radiopharmaceutical to the array of emerging agents for imaging prostate cancer.

Experimental Section

General Procedures. Solvents and chemicals obtained from commercial sources were of analytical grade or better and used without further purification. All experiments were performed in duplicate or triplicate to ensure reproducibility. Analytical thin-layer chromatography (TLC) was performed using Aldrich aluminum-backed 0.2 mm silica gel Z19, 329-1 plates and

visualized by ultraviolet light (254 nm), I_2, and 1% ninhydrin in EtOH. Flash chromatography was performed using silica gel purchased from Bodman (Aston PA), MP SiliTech 32-63 D 60 Å. ^{1}H NMR spectra were recorded on a Bruker Ultrashield 400 MHz spectrometer. Chemical shifts (δ) are reported in ppm downfield by reference to proton resonances resulting from incomplete deuteration of the NMR solvent. Low resolution ESI mass spectra were obtained on a Bruker Daltonics Esquire 3000 Plus spectrometer. High resolution mass spectra were obtained at the University of Notre Dame Mass Spectrometry and Proteomics Facility, Notre Dame, IN, using ESI either by direct infusion on a Bruker micrOTOF-II or by LC elution via an ultrahigh pressure Dionex RSLC with a C18 column coupled with a Bruker micrOTOF-Q II. High-performance liquid chromatographic purification of new compounds, **3**, [$^{69/71}$Ga]**3**, **6**, [$^{69/71}$Ga]**6**, and [^{68}Ga]**3**, was performed using a Phenomenex C_{18} Luna 10 × 250 mm^2 column on a Waters 600E Delta LC system with a Waters 486 tunable absorbance UV/vis detector, both controlled by Empower software. For purification of radiolabeled [^{68}Ga]**6**, a Varian Microsorb-Mv C_{18} 250 × 4.6 mm^2 column was used. HPLC was performed using the following isocratic conditions. For method 1, the mobile phase was 80% solvent A (0.1% TFA in water) and 20% solvent B (0.1% TFA in CH_3CN), flow rate of 4 mL/min. For method 2, the mobile phase was 80% solvent A and 20% solvent B, flow rate of 1 mL/min. Method 1 was used for purification of compounds **3**, [$^{69/71}$Ga]**3**, **6**, [$^{69/71}$Ga]**6**, and [^{68}Ga]**3**. For purification of [^{68}Ga]**6**, method 2 was used. For radiosynthetic purification, HPLC was performed on a Varian Prostar System (Palo Alto, CA) equipped with a model 490 UV absorbance detector and a Bioscan NaI scintillation detector connected to a Bioscan Flow-Count system. All final compounds were obtained in >95% purity, as determined by HPLC.

2-{3-[5-(7-{1-Benzyloxycarbonyl-5-[2-(4,7,10-tris-carboxymethyl-1,4,7,10-tetraazacyclododec-1-yl)acetylamino]pentylcarbamoyl}heptanoylamino)-1-carboxypentyl]ureido}pentanedioic Acid, 3. Compound **3** was prepared in three steps according to Scheme 1. Compound **1** was prepared according to a literature method.[16] To a solution of **1** (100 mg, 0.11 mmol in 5 mL of DMF) was added H-Lys(Boc)-OBz (36 mg, 0.11 mmol).[18] The solution was stirred for 16 h at ambient temperature. The solvent was removed under vacuum. The solid residue thus obtained was dissolved in 10 mL of ethyl acetate and extracted with 3 × 10 mL of water. The organic layer was dried under vacuum to provide a colorless solid. ESIMS: 1154 [M + 1]$^+$. This crude compound was dissolved in 3 mL of $CHCl_3$ followed by addition of 3 mL of TFA at 0 °C. The solution was allowed to stir overnight at ambient temperature. The volume of the solution was reduced under vacuum, and the solid residue was washed with 3 × 5 mL of CH_2Cl_2 to remove impurities. The colorless solid residue, **2**, was dried under vacuum. The crude yield for **2** was 80 mg. Compound **2** was purified further by using a 2 g Sep Pak C18 cartridge with a solution of 85/15 water/acetonitrile (0.1% TFA in each). ^{1}H NMR (D_2O, δ): 7.5 (bm, 5H, Ph), 5.12 (s, 2H, $PhCH_2$), 4.27 (m, 1H, $HC(NH)CO_2$(Glu)), 4.16 (m, 1H, $HC(NH)CO_2$(Lys)), 3.99 (m, 1H, $HC(NH)CO_2$(Lys-linker)), 3.08 (m, 4H, H_2CNH(Lys), H_2CNH(Lys-linker)), 2.39(t, 2H, H_2CCO-linker), 2.21 (m, 2H, H_2CCO_2(Glu)), 2.19 (t, 2H, H_2CCO-linker), 1.89−1.57 (m, 6H, H_2CCH(Glu), H_2CCH(Lys), H_2CCH(Lys-linker)), 1.43−1.16 (m, 16H, $(CH_2)_2$(Lys), $(CH_2)_2$(Lys-linker), $(CH_2)_4$ (linker)). ESIMS: 694 [M + 1]$^+$.

To a solution of DOTA-mono-NHS (54 mg, 0.11 mmol in 5 mL of DMF) was added **2** (80 mg, 0.08 mmol) and TEA (60 μL, 0.43 mmol), and the solution was allowed to stir for 16 h at ambient temperature. Solvent was removed under vacuum, and the crude solid, **3**, was purified by HPLC method 1, retention time 19 min. Yield: ~40%. ^{1}H NMR (D_2O) δ: 7.88 (m, 5H, Ph), 5.10 (s, 2H, H_2CPh), 4.26 (m, 1H, $HC(NH)CO_2$(Glu)), 4.16(m, 1H, $HC(NH)CO_2$(Lys)), 4.06 (m, 1H, $HC(NH)CO_2$(Lys-linker), 3.66 (m, 8H, H_2CCO_2), 3.18 (m, 20H, $N(CH_2)_2N$(DOTA), H_2CNH(Lys), H_2CNH(Lys-linker)), 2.39(t, 2H, H_2CCO-linker), 2.15 (m, 2H, H_2CCO_2(Glu)), 2.07(t, 2H, H_2CCONH-linker), 1.85−1.55(m, 6H, H_2CCH(Glu), H_2CCH(Lys), H_2CCH(Lys-linker)), 1.41−1.14 (m, 16H, $(CH_2)_2$(Lys), $(CH_2)_2$(Lys-linker), $(CH_2)_4$ (linker). ^{13}C NMR (D_2O) δ: 177.8 (CO_2H), 177.6 (CO_2H), 177.5 (CO_2H), 177.1 (CO_2H), 176.3 (CO_2H), 174.2(CO_2CH_2Ph), 173.9 (CONH), 159.8,(NHCONH), 135.5 (C, Ph), 128.9(CH, Ph), 128.5 (CH, Ph),128.1(CH, Ph), 67.3 (CH_2Ph), 55.5 (CH_2CO_2H), 53.4 (CH, Glu), 53.2, 53.1 (CH, Lys, Lys-linker), 52.5, 52.3 (CH_2, DOTA), 39.0 (CH_2NH, Lys), 38.9 (CH_2NH, Lys-linker), 35.5 (CH_2CO, linker), 35.4 (CH_2CO, linker), 30.7(CH_2CO, (Glu)), 28.0 (CH_2CH (Glu)), 27.4, 27.3, 27.1, 26.4, 25.1 (CH_2 (linker), (Lys), (Lys-linker)), 22.3, 22.2(CH_2-(Lys), CH_2(Lys-linker)). ESIMS: 1080 [M + 1]$^+$. HRESI$^+$-MS: calcd for $C_{49}H_{77}N_9O_{18}$, 1080.5487 [M + H]; found, 1080.5459.

2-{3-[5-(7-{1-Benzyloxycarbonyl-5-[2-(4,7,10-tris-carboxymethyl-1,4,7,10-tetraazacyclododec-1-yl)acetylamino]pentylcarbamoyl}heptanoylamino)-1-carboxypentyl]ureido}pentanedioic Acid Gallium-(III), [$^{69/71}$Ga]3. To a solution of $GaNO_3$ (5 mg, 20 μmol) in deionized water was added compound **3** (20 mg, 20 μmol) in 1 mL of deionized water. The resulting solution was heated in boiling water for 10 min. The solvent was evaporated to dryness, and the crude residue was purified by HPLC method 1. Retention time for the product was 24 min. Yield: ~35%. ^{1}H NMR (D_2O) δ: 7.87 (m, 5H, Ph), 5.21 (s, 2H, H_2CPh), 4.26−4.1 (m, 3H, $HC(NH)CO_2$(Glu), $HC(NH)CO_2$(Lys), $HC(NH)CO_2$(Lys-linker)), 3.45 −3.18 (bm, 28H, H_2CCO_2, $N(CH_2)_2N$(DOTA), H_2CNH-(Lys), H_2CNH(Lys-linker)), 2.42 (m, 2H, H_2C-linker), 2.20 (m, 2H, H_2CCO_2(Glu), 2.06 (m, 3H, H_2C-linker, H_2CCH(Glu)), 1.85−1.18 (m, 21H, H_2CCH(Glu), H_2C(Lys), H_2C(Lys-linker), $(CH_2)_4$ (linker)). ^{13}C NMR (D_2O) δ: 178.2 (CO_2H), 178.1 (CO_2H), 177.9 (CO_2H), 177.5 (CO_2H), 177.4 (CO_2H) 176.3 (CO_2H), 174.5(CO_2CH_2Ph), 173.9, 173.4 (CONH), 160.1 (NH-CONH), 135.6 (C, Ph), 129.1(CH, Ph), 128.9 (CH, Ph), 128.1(CH, Ph), 67.3 (CH_2Ph), 60.1, 59.6, 57.6, 57.3 (CH_2CO_2H), 53.4 (CH, Glu), 53.2, 53.1 (CH, Lys, Lys-linker), 52.9, 52.8, 52.5 (CH_2, DOTA), 39.0, 38.9 (CH_2NH, Lys, Lys-CH_2), 35.7, 35.5 (CH_2CO, linker), 31.1 (CH_2CO, Glu), 27.9 (CH_2CH)), 27.7, 27.6, 27.5, 26.4, 25.1 (linker, CH_2(Lys), CH_2(Lys-linker), 22.3, 22.2 (CH_2(Lys), CH_2(Lys-linker)). ESIMS m/z: 1146 [M + H]$^+$. HRESI$^+$-MS: calcd for $C_{49}H_{75}GaN_9O_{18}$, 1146.4486 [M + H]; found, 1146.4480.

2-[3-(1-Carboxy-5-{7-[5-carboxy-5-(3-phenyl-2-{3-phenyl-2-[2-(4,7,10-tris-carboxymethyl-1,4,7,10-tetraazacyclododec-1-yl)acetylamino]propionylamino}propionylamino)pentylcarbamoyl]heptanoylamino}pentyl)ureido]pentanedioic Acid, 6. Fmoc-Lys-(Boc)-Wang resin (100 mg, 0.09 mM) was allowed to swell with CH_2Cl_2 (3 mL) followed by DMF (3 mL). A solution of 20% piperidine in DMF (3 mL) was added to the resin that was then shaken gently on a mechanical shaker for 30 min at ambient temperature. The resin was washed with DMF (3 × 3 mL) and CH_2Cl_2 (3 × 3 mL). Formation of free amine was assessed by the Kaiser test.[42] After the resin was swelled in DMF, a solution of Fmoc-Phe-OH (3 equiv), HBTU (3 equiv), HOBt (3 equiv), and DIPEA (4.0 equiv) in DMF was added and gently shaken for 2 h. The resin was then washed with DMF (3 × 3 mL) and CH_2Cl_2 (3 × 3 mL). The coupling efficiency was assessed by the Kaiser test. That aforementioned sequence was repeated for two more coupling steps with Fmoc-Phe-OH and DOTA-(*tert*-butyl ester)$_3$-CO_2H. Final compound was cleaved from the resin using TFA/CH_2Cl_2 (1:1) and concentrated under vacuum to produce **4**. The concentrated product was purified by using a C18 SepPak Vac 2 g column. The product was eluted with a solution 70/30 water/acetonitrile (0.1% TFA in each). ^{1}H NMR (D_2O, δ): 7.14−7.00 (m, 10H, Ph), 4.51 (m, 1H, HC(Phe)), 4.42 (m, 1H, HC(Phe)), 4.04 (m, 1H, HC(Lys)), 3.16−2.4 (bm, 30H, H_2CCO_2, $N(CH_2)_2N$-(DOTA), H_2CPh(Phe), H_2CNH(Lys)), 1.61−1.39 (m, 4H, H_2C (Lys)), 1.16 (m, 2H, H_2C(Lys)). ^{13}C NMR (D_2O) δ: 174.8 (CO_2H), 172.24 (CONH), 172 (CONH), 136.5 (C, Phe), 135.8 (C, Phe), 129.3 (CH, Phe), 128.5 (CH, Phe), 126.9 (CH, Phe), 54.6 (CH_2-CO_2), 53.07 (CH, Phe, Lys), 52.1−51.0 (CH_2, DOTA), 39.06

(CH_2NH_2(Lys), 36.32 (CH_2Ph), 29.61 (CH_2, Lys), 26.0 (CH_2, Lys), 21.73, (CH_2, Lys). ESIMS: 827 $[M + 1]^+$.

Lyophilized **4** (10 mg, 12 μmol in 2 mL DMF) was added to **5**[19] (20 mg, 21.4 μmol in 1 mL of DMF) followed by TEA (214 μmol, 30 μL) and then stirred at 25 °C for 16 h. After solvent removal, solid residue was treated with 3 mL of TFA/CH_2Cl_2 to remove the PMB group. The residue was washed with 2 × 5 mL of CH_2Cl_2 to remove impurities. The colorless solid residue, compound **6**, thus obtained was purified by a C18 SepPak Vac 2 g column using an eluent of 70/30 water/acetonitrile (0.1% TFA in each). The product was further purified using preparative RP-HPLC by method 1, retention time 17 min. Yield: ~30%. ^{1}H NMR (CD_3CO_2D) δ: 7.35−7.20 (m, 10H, Ph), 4.86 (bm, 2H, HC(Phe)), 4.57−4.46 (3H, HC(NH)CO_2(Glu), HC(NH)CO(Lys), HC(NH)CO(Lys-linker)), 4.4−3.0 (m, 30H, H_2CCO_2, N$(CH_2)_2$N(DOTA), H_2CPh(Phe), H_2CNH(Lys), H_2CNH(Lys-linker)), 2.8 (m, 2H, H_2CPh(Phe)), 2.6 (m, 2H, H_2CCO_2(Glu)), 2.3 (m, 5H, H_2CCHNH(Glu), H_2CCONH-linker)), 2.1−1.3 (m, 21H, H_2CCHNH(Glu), $(CH_2)_4$-linker, $(CH_2)_3$(Lys), $(CH_2)_3$(Lys-linker)). ^{13}C NMR (CD_3CO_2D) δ: 178.71, (CO_2H), 178.14 (CO_2H), 177.72 (CO_2H), 177.66 (CO_2H), 177.06 (CO_2H), 174.24 (CONH), 173.9 (CONH), 161.3 (NHCONH), 138.6 (C, Ph) 137.7(C, Ph), 130.5 (CH, Ph), 129.5 (CH, Ph), 127.9 (CH, Ph), 127.7 (CH, Ph), 56.72 (CH_2CO_2), 56.16 (CH, Phe), 54.6 (CH, Glu), 53.5 (CH, Lys, Lys-linker), 53.3 (CH_2, DOTA), 40.8 (CH_2NH (Lys)), 39.4 (CH_2NH, (Lys-linker)), 37.5 (CH_2Phe), 32.6 (CH_2, (linker)) 31.8 (CH_2, (linker)), 30.7, 29.42, 27.9, 26.53 (CH_2 (linker), CH_2(Lys)). ESIMS m/z: 1284 $[M + H]^+$. HRESI$^+$-MS: calcd for $C_{68}H_{90}N_{11}O_{20}$, 1284.6365 [M + H]; found, 1284.6358.

2-[3-(1-Carboxy-5-{7-[5-carboxy-5-(3-phenyl-2-{3-phenyl-2-[2-(4,7,10-tris-carboxymethyl-1,4,7,10-tetraazacyclododec-1-yl)acetylamino]propionylamino}propionylamino)pentylcarbamoyl]heptanoylamino}pentyl)ureido]pentanedioic Acid Gallium(III), [$^{69/71}$Ga]6. This compound was prepared according to the same general procedure as described for [$^{69/71}$Ga]**3**. Compound [$^{69/71}$Ga]**6** was purified by method 1, retention time 22 min. Yield: ~30%. ^{1}H NMR (MeOD) δ: 7.30−7.20 (m, 10H, Ph), 4.76−4.67(bm, 2H, HC(Phe)), 4.36−4.27 (3H, HC(NH)CO_2(Glu), HC(NH)CO_2-(Lys), HC(NH)CO(Lys-linker)), 4.0−3.35 (m, 24H, H_2CCO_2, N$(CH_2)_2$N(DOTA)), 3.29−3.1 (m, 5H, H_2CPh(Phe), H_2CNH-(Lys), H_2CNH(Lys-linker)), 3.05 (m, 1H, H_2CNH(Lys)), 2.27 (m, 2H, H_2CPh(Phe)), 2.4 (m, 2H, H_2CCONH-linker), 2.28−2.1 (m, 5H, H_2CCO_2(Glu), H_2CCHNH(Glu), H_2CCONH-linker)), 1.98−1.8 (3H, H_2CCHNH(Glu), CH_2-linker), 1.8−1.3 (m, 18H, $(CH_2)_4$-linker, $(CH_2)_3$-Lys, $(CH_2)_3$-Lys-linker)). ^{13}C NMR (MeOD) δ: 175.71 (CO_2H), 174.4 (CO_2H), 174.2 (CO_2H), 173.2 (CO_2H), 171.9 (CO_2H), 170.4 (CONH), 170.3, 170.2, 169.9 (CONH), 169.5 (CONH), 159.0 (NHCONH), 137.3 (C, Ph) 136.9 (C, Ph), 129.3 (CH, Ph), 129.2 (CH, Ph), 128.3 (CH, Ph), 128.2 (CH, Ph), 126.3, 126.2 (CH, Ph), 61.8, 60.7, 59.4, 59.3 (CH_2CO_2), 57.6 (CH, (Glu)), 57.5 (CH, (Lys), (Lys-linker)), 54.4, 54.3 (CH(Phe)), 54.2, 54.1, 52.8, 52.5, 52.3 (CH_2, DOTA), 37.5, 37.4 (CH_2NH, (Lys-linker), Lys), 35.5 (CH_2Phe), 35.4 (CH_2Phe), 32.0 (CH_2CO_2, Glu), 30.8 (CH_2CONH, linker), 29.7 (CH_2CH, Glu), 29.42, 29.3, 29, 7, 27.9, 26.53, 22.5, 22.3 (CH_2(linker), CH_2-(Lys), CH_2(Lys-linker)). ESIMS m/z: 1351$[M + H]^+$. HRESI$^+$-MS: calcd for $C_{68}H_{86}GaN_{11}NaO_{20}$, 1372.5204 $[M + Na]^+$; found, 1372.5199.

Preparation of ^{68}Ga. ^{68}Ga labeling of compounds [^{68}Ga]**3** and [^{68}Ga]**6** were performed according to a literature procedure.[24] A detailed description for [^{68}Ga]**3** is given below.

Preconcentration of [^{68}Ga(III)]. A sample of 488 MBq (13 mCi) of $^{68}GaCl_3$ in 7 mL of 0.1 N HCl was obtained from an 18-month-old 1850 MBq (50 mCi) ^{68}Ge/^{68}Ga generator, Eckert-Ziegler (Berlin). The solution was transferred on a cation-exchange cartridge, Phenomenex Strata-X-C (33 μm strong cation exchange resin, part no. 8B-S029-TAK, 30 mg/1 mL). The column was eluted with 5 mL of a solution of 20/80 of hydrochloric acid (0.10 N)/acetone. The eluent remaining on the cation exchanger was removed by passage of nitrogen. That process was performed to remove most of the remaining chemical and radiochemical impurities from the resin, whereas ^{68}Ga(III) should remain on the column. The column was filled with 150 μL of a 2.4/97.6 HCl (0.05 N)/acetone solution. About 2 min standing appeared to be best for complete desorption of the ^{68}Ga(III) from the resin into the liquid phase. An additional 250 μL of that 2.4/97.6 HCl (0.05 N)/acetone solution was applied, and the purified ^{68}Ga(III) was obtained in a total volume of 400 μL.

General Radiolabeling Procedure. The 400 μL combined fractions of ^{68}Ga(III) in HCl/acetone was used directly for the radiolabeling of **3**/**6**. The concentrated radioactivity was added to 500 μL of deionized H_2O in a standard glass reagent vial containing 100 μL (92 nmol, 1 mg/mL solution) of ligand. No buffer solution was added. The reaction vial was heated at 95 °C for 10 min. The complexation was monitored by injecting aliquots of 100 μL (7.77 MBq) of the solution onto the HPLC. Product obtained was 5.92 MBq. For [^{68}Ga]**3**, radiochemical yield was 76.2% (without decay correction) and the radiochemical purity was >99%. HPLC was performed by method 1 as described in the Experimental Section. t_R = 25 min for the desired product and t_R = 19 min for the free ligand. For [^{68}Ga]**6**, radiochemical yield was 70% and radiochemical purity was >99%. HPLC was performed by method 2 as stated in the Experimental Section. t_R = 22.5 min for the desired product and t_R = 16 min for the free ligand. The acidic eluate was neutralized with 100 μL of 0.1 M $NaHCO_3$ solution, and the volume of the eluate was reduced under vacuum to dryness. The solid residue was diluted with saline to the desired radioactivity concentration for biodistribution and imaging studies.

Lipophilicity Determination. Partition coefficients, $\log_{o/w}$ (pH 7.4) values, were determined according to a literature procedure.[25] Briefly, a solution of either [^{68}Ga]**3** or [^{68}Ga]**6** was added to a presaturated solution of 1-octanol (5 mL) mixed with phosphate buffered saline (PBS) (5 mL) in a 15 mL centrifuge tube. After the mixture was vigorously shaken, it was centrifuged at 3000 rpm for 5 min. Aliquots (100 μL) were removed from the two phases, and the radioactivity was measured in a γ-counter, 1282 Compugamma CS (LKB, Wallac, Turku, Finland).

Cell Lines and Tumor Models. PC-3 PIP (PSMA+) and PC-3 flu (PSMA−) cell lines were obtained from Dr. Warren Heston (Cleveland Clinic) and were maintained as previously described.[13] LNCaP cells were obtained from American Type Culture Collection (ATCC, Manassas, VA) and were maintained as per ATCC guidelines. All cells were grown to 80−90% confluence before trypsinization and formulation in Hank's balanced salt solution (HBSS, Sigma, St. Louis, MO) for implantation into mice.

Animal studies were undertaken in compliance with institutional guidelines related to the conduct of animal experiments. For biodistribution studies of [^{68}Ga]**3** and [^{68}Ga]**6** and imaging studies of [^{68}Ga]**3**, male SCID mice (NCI) were implanted subcutaneously with (1−5) × 10^6 PSMA+ PC-3 PIP and PSMA− PC-3 flu cells behind either shoulder. For imaging studies of [^{68}Ga]**3**, male SCID mice (NCI) were implanted subcutaneously with 5 × 10^6 LNCaP cells behind the right shoulder. Mice were imaged or used in biodistribution studies when the tumor xenografts reached 3−5 mm in diameter.

Biodistribution. PSMA+ PC-3 PIP and PSMA− PC-3 flu xenograft-bearing SCID mice were injected via the tail vein with 30 μCi (1.1 MBq) [^{68}Ga]**3** or [^{68}Ga]**6**. In case each four mice were sacrificed by cervical dislocation at 30, 60, 120, 180 min pi for [^{68}Ga]**3** and at 5, 60, 120, 180 min pi for [^{68}Ga]**6**. The heart, lungs, liver, stomach, pancreas, spleen, fat, kidney, muscle, small and large intestines, urinary bladder, and PC-3 PIP and flu tumors were quickly removed. A 0.1 mL sample of blood was also collected. Each organ was weighed, and the tissue radioactivity was measured with an automated γ counter (1282

Compugamma CS, Pharmacia/LKB Nuclear, Inc., Gaithersburg, MD). The %ID/g was calculated by comparison with samples of a standard dilution of the initial dose. All measurements were corrected for decay.

PET and CT Imaging. A single SCID mouse implanted with a PSMA+ LNCaP xenograft was injected intravenously with 0.2 mCi (7.4 MBq) [^{68}Ga]**3** in 200 μL of 0.9% NaCl. At 0.5 h pi, the mouse was anesthetized with 3% isoflurane in oxygen for induction and maintained under 1.5% isoflurane in oxygen at a flow rate of 0.8 L/min. The mouse was positioned in the prone position on the gantry of a GE eXplore VISTA small animal PET scanner (GE Healthcare, Milwaukee, WI). Image acquisition was performed using the following protocol. The images were acquired as a pseudodynamic scan; i.e., a sequence of successive whole-body images were acquired in three bed positions for a total of 120 min. The dwell time at each position was 5 min such that a given bed position (or mouse organ) was revisited every 15 min. An energy window of 250−700 keV was used. Images were reconstructed using the FORE/2D-OSEM method (two iterations, 16 subsets) and included correction for radioactive decay, scanner dead time, and scattered radiation. After PET imaging, the mobile mouse holder was placed on the gantry of an X-SPECT (Gamma Medica Ideas, Northridge, CA) small animal imaging device to acquire the corresponding CT. Animals were scanned over a 4.6 cm field-of-view using a 600 μA, 50 kV beam. The PET and CT data were then co-registered using Amira 5.2.0 software (Visage Imaging Inc., Carlsbad, CA).

Imaging studies and blocking studies of [^{68}Ga]**6** and [^{68}Ga]**3** were carried out on PSMA+ PC-3 PIP and PSMA− PC-3 flu xenograft-bearing SCID mice or PSMA+ PC-3 PIP (25.9 MBq in 100 μL of NaCl) xenograft-bearing SCID mice. At 30 min, 1 h, and 2 h pi the mice were anesthetized and whole-body images were obtained using the PET scanner as mentioned above, in two bed positions, 15 min at each position for a total of 30 min using the same energy window. Images were reconstructed and co-registered with the corresponding CT images using the same methods as described above.

Acknowledgment. We thank Dr. Richard L. Wahl for provision of the ^{68}Ga generator. We also thank NIH (Grants R01 CA134675 and U24 CA92871) and the AdMeTech Foundation for financial support.

Supporting Information Available: HPLC traces and high-resolution mass spectra for [^{68}Ga]**3** and [^{68}Ga]**6**; a figure containing a PET blocking study for [^{68}Ga]**3**. This material is available free of charge via the Internet at http://pubs.acs.org.

References

(1) *Cancer Facts & Figures*; American Cancer Society: Atlanta, GA, 2009.
(2) Ghosh, A.; Heston, W. D. Tumor target prostate specific membrane antigen (PSMA) and its regulation in prostate cancer. *J. Cell. Biochem.* **2004**, *91*, 528–539.
(3) Milowsky, M. I.; Nanus, D. M.; Kostakoglu, L.; Sheehan, C. E.; Vallabhajosula, S.; Goldsmith, S. J.; Ross, J. S.; Bander, N. H. Vascular targeted therapy with anti-prostate-specific membrane antigen monoclonal antibody J591 in advanced solid tumors. *J. Clin. Oncol.* **2007**, *25*, 540–547.
(4) Kowol, C. R.; Berger, R.; Eichinger, R.; Roller, A.; Jakupec, M. A.; Schmidt, P. P.; Arion, V. B.; Keppler, B. K. Gallium(III) and iron(III) complexes of alpha-N-heterocyclic thiosemicarbazones: synthesis, characterization, cytotoxicity, and interaction with ribonucleotide reductase. *J. Med. Chem.* **2007**, *50*, 1254–1265.
(5) Kowol, C. R.; Trondl, R.; Heffeter, P.; Arion, V. B.; Jakupec, M. A.; Roller, A.; Galanski, M.; Berger, W.; Keppler, B. K. Impact of metal coordination on cytotoxicity of 3-aminopyridine-2-carboxaldehyde thiosemicarbazone (triapine) and novel insights into terminal dimethylation. *J. Med. Chem.* **2009**, 5032–5043.
(6) Kaluderovic, M. R.; Gomez-Ruiz, S.; Gallego, B.; Hey-Hawkins, E.; Paschke, R.; Kaluderovic, G. N. Anticancer activity of dinuclear gallium(III) carboxylate complexes. *Eur. J. Med. Chem.* **2010**, *45*, 519–525.
(7) Fani, M.; Andre, J. P.; Maecke, H. R. ^{68}Ga-PET: a powerful generator-based alternative to cyclotron-based PET radiopharmaceuticals. *Contrast Media Mol. Imaging* **2008**, *3*, 67–77.
(8) Khan, M. U.; Khan, S.; El-Refaie, S.; Win, Z.; Rubello, D.; Al-Nahhas, A. Clinical indications for gallium-68 positron emission tomography imaging. *Eur. J. Surg. Oncol.* **2009**, *35*, 561–567.
(9) Sanchez-Crespo, A.; Andreo, P.; Larsson, S. A. Positron flight in human tissues and its influence on PET image spatial resolution. *Eur. J. Nucl. Med. Mol. Imaging* **2004**, *31*, 44–51.
(10) Reubi, J. C.; Maecke, H. R. Peptide-based probes for cancer imaging. *J. Nucl. Med.* **2008**, *49*, 1735–1738.
(11) Chen, Y.; Foss, C. A.; Byun, Y.; Nimmagadda, S.; Pullambhatla, M.; Fox, J. J.; Castanares, M.; Lupold, S. E.; Babich, J. W.; Mease, R. C.; Pomper, M. G. Radiohalogenated prostate-specific membrane antigen (PSMA)-based ureas as imaging agents for prostate cancer. *J. Med. Chem.* **2008**, *51*, 7933–7943.
(12) Foss, C. A.; Mease, R. C.; Fan, H.; Wang, Y.; Ravert, H. T.; Dannals, R. F.; Olszewski, R. T.; Heston, W. D.; Kozikowski, A. P.; Pomper, M. G. Radiolabeled small-molecule ligands for prostate-specific membrane antigen: in vivo imaging in experimental models of prostate cancer. *Clin. Cancer Res.* **2005**, *11*, 4022–4028.
(13) Mease, R. C.; Dusich, C. L.; Foss, C. A.; Ravert, H. T.; Dannals, R. F.; Seidel, J.; Prideaux, A.; Fox, J. J.; Sgouros, G.; Kozikowski, A. P.; Pomper, M. G. *N*-[*N*-[(*S*)-1,3-dicarboxypropyl]carbamoyl]-4-[^{18}F]fluorobenzyl-L-cysteine, [^{18}F]DCFBC: a new imaging probe for prostate cancer. *Clin. Cancer Res.* **2008**, *14*, 3036–3043.
(14) Kularatne, S. A.; Zhou, Z.; Yang, J.; Post, C. B.; Low, P. S. Design, synthesis, and preclinical evaluation of prostate-specific membrane antigen targeted (99m)Tc-radioimaging agents. *Mol. Pharmaceutics* **2009**, *6*, 790–800.
(15) Kularatne, S. A.; Wang, K.; Santhapuram, H-K., R.; Low, P. S. Prostate-specific membrane antigen (PSMA)-targeted imaging and therapy of prostate cancer using a PSMA inhibitor as a homing ligand. *Mol. Pharmaceutics* **2009**, *6*, 780–789.
(16) Banerjee, S. R.; Foss, C. A.; Castanares, M.; Mease, R. C.; Byun, Y.; Fox, J. J.; Hilton, J.; Lupold, S. E.; Kozikowski, A. P.; Pomper, M. G. Synthesis and evaluation of technetium-99m- and rhenium-labeled inhibitors of the prostate-specific membrane antigen (PSMA). *J. Med. Chem.* **2008**, *51*, 4504–4517.
(17) Clarke, E. T. M. Stabilities of trivalent metal ion complexes of the tetraacetate derivatives of 12-, 13-, and 14-membered tetraazamacrocycles. *Inorg. Chim. Acta* **1992**, *190*, 37–46.
(18) Hamachi, I, Y. Y.; Matsugi, T; Shinkai, S. Single- or dual-mode switching of semisynthetic ribonuclease S′ with an iminodiacetic acid moiety in response to the copper(II) concentration. *Chem.—Eur. J.* **1999**, *5*, 1503–1511.
(19) Chandran, S. S.; Banerjee, S. R.; Mease, R. C.; Pomper, M. G.; Denmeade, S. R. Characterization of a targeted nanoparticle functionalized with a urea-based inhibitor of prostate-specific membrane antigen (PSMA). *Cancer Biol. Ther.* **2008**, *7*, 974–982.
(20) Heppeler, A.; Andre, J. P.; Buschmann, I.; Wang, X.; Reubi, J.-C.; Hennig, M.; Kaden, T. A.; Maecke, H. R. Metal-ion-dependent biological properties of a chelator-derived somatostatin analogue for tumor targeting. *Chem.—Eur. J.* **2008**, *14*, 3026–3034.
(21) Heppeler, A.; Froidevaux, S.; Maecke, H. R.; Jermann, E.; Behe, M.; Powell, P.; Hennig, M. Radiometal-labelled macrocyclic chelator-derivatized somatostatin analogue with superb tumour-targeting properties and potential for receptor-mediated internal radiotherapy. *Chem.—Eur. J.* **1999**, *5*, 1974–1981.
(22) Viola, N. A.; Rarig, R. S.; Ouellette, W.; Doyle, R. P. Synthesis, structure and thermal analysis of the gallium complex of 1,4,7,10-tetraazacyclododecane-*N*,*N*′,*N*″,*N*‴-tetraacetic acid (DOTA). *Polyhedron* **2006**, *25*, 3457–3462.
(23) Henderson, W.; Taylor, M. J. An electrospray mass spectrometric investigation of gallium trihalide and indium trihalide solutions. *Inorg. Chim. Acta* **1998**, *277*, 26–30.
(24) Zhernosekov, K. P.; Filosofov, D. V.; Baum, R. P.; Aschoff, P.; Bihl, H.; Razbash, A. A.; Jahn, M.; Jennewein, M.; Rosch, F. Processing of generator-produced ^{68}Ga for medical application. *J. Nucl. Med.* **2007**, *48*, 1741–1748.
(25) Antunes, P.; Ginj, M.; Walter, M. A.; Chen, J.; Reubi, J. C.; Maecke, H. R. Influence of different spacers on the biological profile of a DOTA-somatostatin analogue. *Bioconjugate Chem.* **2007**, *18*, 84–92.
(26) Kozikowski, A. P.; Zhang, J.; Nan, F.; Petukhov, P. A.; Grajkowska, E.; Wroblewski, J. T.; Yamamoto, T.; Bzdega, T.; Wroblewska, B.; Neale, J. H. Synthesis of urea-based inhibitors as active site probes of glutamate carboxypeptidase II: efficacy as analgesic agents. *J. Med. Chem.* **2004**, *47*, 1729–1738.
(27) Chang, S. S.; Reuter, V. E.; Heston, W. D.; Bander, N. H.; Grauer, L. S.; Gaudin, P. B. Five different anti-prostate-specific membrane

antigen (PSMA) antibodies confirm PSMA expression in tumor-associated neovasculature. *Cancer Res*. **1999**, *59*, 3192–3198.
(28) Silver, D. A.; Pellicer, I.; Fair, W. R.; Heston, W. D.; Cordon-Cardo, C. Prostate-specific membrane antigen expression in normal and malignant human tissues. *Clin. Cancer Res*. **1997**, *3*, 81–85.
(29) Slusher, B. S.; Tsai, G.; Yoo, G.; Coyle, J. T. Immunocytochemical localization of the *N*-acetyl-aspartyl-glutamate (NAAG) hydrolyzing enzyme N-acetylated alpha-linked acidic dipeptidase (NAALADase). *J. Comp. Neurol*. **1992**, *315*, 217–229.
(30) Caroli, P.; Nanni, C.; Rubello, D.; Alavi, A.; Fanti, S. Non-FDG PET in the practice of oncology. *Indian J. Cancer* **2010**, *47*, 120–125.
(31) Hao, G.; Zhou, J.; Guo, Y.; Long, M. A.; Anthony, T.; Stanfield, J.; Hsieh, J. T.; Sun, X. A cell permeable peptide analog as a potential-specific PET imaging probe for prostate cancer detection. *Amino Acids* [Online early access]. DOI: 10.1007/s00726-010-0515-5. Published Online: Mar 10, 2010.
(32) Lapi, S. E.; Wahnishe, H.; Pham, D.; Wu, L. Y.; Nedrow-Byers, J. R.; Liu, T.; Vejdani, K.; VanBrocklin, H. F.; Berkman, C. E.; Jones, E. F. Assessment of an ^{18}F-labeled phosphoramidate peptidomimetic as a new prostate-specific membrane antigen-targeted imaging agent for prostate cancer. *J. Nucl. Med*. **2009**, *50*, 2042–2048.
(33) Dimitrakopoulou-Strauss, A.; Hohenberger, P.; Haberkorn, U.; Macke, H. R.; Eisenhut, M.; Strauss, L. G. ^{68}Ga-labeled bombesin studies in patients with gastrointestinal stromal tumors: comparison with ^{18}F-FDG. *J. Nucl. Med*. **2007**, *48*, 1245–1250.
(34) Henze, M.; Dimitrakopoulou-Strauss, A.; Milker-Zabel, S.; Schuhmacher, J.; Strauss, L. G.; Doll, J.; Macke, H. R.; Eisenhut, M.; Debus, J.; Haberkorn, U. Characterization of ^{68}Ga-DOTA-D-Phe1-Tyr3-octreotide kinetics in patients with meningiomas. *J. Nucl. Med*. **2005**, *46*, 763–769.
(35) Henze, M.; Schuhmacher, J.; Dimitrakopoulou-Strauss, A.; Strauss, L. G.; Macke, H. R.; Eisenhut, M.; Haberkorn, U. Exceptional increase in somatostatin receptor expression in pancreatic neuroendocrine tumour, visualised with (68)Ga-DOTA-TOC PET. *Eur. J. Nucl. Med. Mol. Imaging* **2004**, *31*, 466.
(36) Prasad, V.; Ambrosini, V.; Hommann, M.; Hoersch, D.; Fanti, S.; Baum, R. P. Detection of unknown primary neuroendocrine tumours (CUP-NET) using (68)Ga-DOTA-NOC receptor PET/CT. *Eur. J. Nucl. Med. Mol. Imaging* **2010**, *37*, 67–77.
(37) Prasad, V.; Baum, R. P. Biodistribution of the Ga-68 labeled somatostatin analogue DOTA-NOC in patients with neuroendocrine tumors: characterization of uptake in normal organs and tumor lesions. *Q. J. Nucl. Med. Mol. Imaging* **2010**, *54*, 61–67.
(38) Putzer, D.; Gabriel, M.; Kendler, D.; Henninger, B.; Knoflach, M.; Kroiss, A.; Vonguggenberg, E.; Warwitz, B.; Virgolini, I. J. Comparison of ^{68}Ga-DOTA-Tyr3-octreotide and ^{18}F-fluoro-L-dihydroxyphenylalanine positron emission tomography in neuroendocrine tumor patients. *Q. J. Nucl. Med. Mol. Imaging* **2010**, *54*, 68–75.
(39) van Essen, M.; Krenning, E. P.; Kam, B. L.; de Herder, W. W.; Feelders, R. A.; Kwekkeboom, D. J. Salvage therapy with (177)Lu-octreotate in patients with bronchial and gastroenteropancreatic neuroendocrine tumors. *J. Nucl. Med*. **2010**, *51*, 383–390.
(40) Barinka, C.; Byun, Y.; Dusich, C. L.; Banerjee, S. R.; Chen, Y.; Castanares, M.; Kozikowski, A. P.; Mease, R. C.; Pomper, M. G.; Lubkowski, J. Interactions between human glutamate carboxypeptidase II and urea-based inhibitors: structural characterization. *J. Med. Chem*. **2008**, *51*, 7737–7743.
(41) Jackson, P. F.; Cole, D. C.; Slusher, B. S.; Stetz, S. L.; Ross, L. E.; Donzanti, B. A.; Trainor, D. A. Design, synthesis, and biological activity of a potent inhibitor of the neuropeptidase N-acetylated alpha-linked acidic dipeptidase. *J. Med. Chem*. **1996**, *39*, 619–622.
(42) Kaiser, E.; Colescott, R. L.; Bossinger, C. D.; Cook, P. I. Color test for detection of free terminal amino groups in the solid-phase synthesis of peptides. *Anal. Biochem*. **1970**, *34*, 595–598.